Natural and Synthetic Xanthones as Monoamine Oxidase Inhibitors: Biological Assay and 3D-QSAR

by **Carmela Gnerre**[a]), **Ulrike Thull**[a]), **Patrick Gaillard**[a]), **Pierre-Alain Carrupt**[a]), **Bernard Testa***[a]), **Eduarda Fernandes**[b]), **Francisco Silva**[b]), **Manuela Pinto**[b]), **Madalena M. M. Pinto**[b]), **Jean-Luc Wolfender**[c]), **Kurt Hostettmann**[c]), and **Gabriele Cruciani**[d])

[a]) Institut de Chimie Thérapeutique, Université de Lausanne, BEP, CH-1015 Lausanne
[b]) Laboratorio de Quimica Organica, Faculdade de Farmacia, rua Anìbal Cunha 164, P-4050 Porto
[c]) Institut de Pharmacognosie et Phytochimie, Université de Lausanne, BEP, CH-1015 Lausanne
[d]) Laboratorio di Chemiometria, Dipartimento di Chimica, Università di Perugia, Via Elce di Sotto 10, I-06123 Perugia

Fifty-nine xanthones (= 9*H*-xanthen-9-ones) of natural or synthetic origin were investigated for their inhibitory activity toward monoamine-oxidase A (MAO-A) and MAO-B. The compounds demonstrated reversible, time-independent activities, with selectivity toward MAO-A. The most active inhibitor had an IC_{50} of 40 nM. Electron absorption spectroscopy revealed the formation of a 1:1 charge-transfer complex between lumiflavine and xanthones. 3D-QSAR Studies according to the CoMFA/GOLPE procedure provided information on the relationship between steric and electrostatic fields and MAO-A inhibition. The ALMOND procedure yielded additional topographical information on structural factors favoring activity.

1. Introduction. – Monoamine oxidase (MAO; E.C. 1.4.3.4.) is an FAD-containing enzyme of the outer mitochondrial membrane that exists as two isoenzymes (MAO-A and MAO-B), which differ in substrate specificity, sensitivity to inhibitors, and primary amino acid sequence. Even if relatively little is known on the topographical differences between the active sites of the two enzymes [1], an important site-directed mutagenesis study [2] has identified a key amino acid responsible for substrate selectivity. Substitution of Phe-208 in MAO-A with the corresponding Ile-199 in MAO-B converted the selectivity profile of the A to the B form, and *vice versa.* Thus, aromatic interactions may be involved in MAO-A binding, whereas hydrophobic and *van der Waals* interactions may be involved in MAO-B binding. Recently, *Moron et al.* [3] have shown through computational simulation of ligand recognition that these amino acids should play a key role also in the selectivity of inhibitors.

There is at present a considerable pharmacological and therapeutic interest in reversible inhibitors of MAO-A and MAO-B [4]. These agents belong to a large variety of chemical classes, *e.g.*, isoquinolines, tetrahydroisoquinolines [5], 4-(2-benzofuranyl)piperidines [6], oxadiazoles [7], phenoxathiin 10,10-dioxides [8], and natural xanthones [9]. The exact mechanism by which they interact with MAO is only partly understood.

Xanthones (= 9*H*-xanthen-9-ones) of natural and synthetic origin are of biological and pharmacological interest. On the one hand, they are of particular importance in chemotaxonomy as systematic markers. On the other hand, they have valuable pharmacological properties, xanthone-containing plant extracts being used in traditional medicine [10].

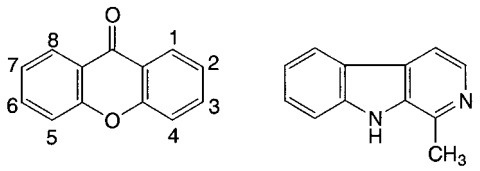

Xanthone Harmane

An important step toward the design of MAO inhibitors is the rationalization and characterization of structural features important for activity. In this study, we present MAO-A and MAO-B inhibitory activities of 59 xanthone derivatives. A spectrophotometric method, with lumiflavine as a model for the FAD cofactor, was applied to study the charge-transfer mechanism of some xanthones. Finally, structure-activity relationship (SAR) studies of MAO-A inhibition were carried out on the basis of two 3D-quantitative structure-activity relationship (3D-QSAR) approaches, namely, Comparative Molecular Field Analysis (CoMFA) in combination with GOLPE for variable selection, and the ALMOND program to obtain alignment-independent descriptors. The MAO-B data presented here were not suitable for 3D-QSAR analysis due to a narrow range of activities.

2. Results and Discussion. – 2.1. *Structure-Activity Relationships.* The majority of compounds acted preferentially as MAO-A inhibitors with IC_{50} values in the micro- to nanomolar range (*Table 1*). Compound **22** (1,5-dihydroxy-3-methoxyxanthone) with an IC_{50} of 40 nM for MAO-A emerged as the most active inhibitor.

A surprising result is the strong activity and selectivity of the unsubstituted compound **1**. Nevertheless, six substituted compounds, namely **2**, **7**, **10**, **13**, **22**, and **40**, were more active toward MAO-A than compound **1**. Even with a limited variety of substituents, some structural features that modulate MAO-A inhibition and selectivity can be seen. Hexasubstitution (**47**–**49**) appears to be an unfavorable feature. In contrast, monosubstitution in positions 1 to 4 led to equipotent (**3**, **4**, **5**, **6**, and **8**) or more active (**2** and **7**) compounds, except for compound **9**, which was significantly less active.

Compounds with an OH group at C(1) were more potent toward MAO-A than compounds with an MeO substituent or *O*-glycosylated compounds (**2** *vs.* **3**, **13** *vs.* **14**, **23** *vs.* **24**; **43** *vs.* **44**). Since compounds bearing an MeO group at C(5) were significantly less active than the corresponding hydroxylated compounds (**11** *vs.* **12**; **22** *vs.* **23**; **33** *vs.* **34**), a small, hydrophilic substituent appears favorable for activity. The opposite was true for position 3. Here, the methoxylated compounds were 4–100 times more active than the hydroxylated ones (**21** *vs.* **22**; **39** *vs.* **40**; **42** *vs.* **43**), except for compound **15** compared to **12**. Although this phenomenon is difficult to explain, some interpretations can be proposed. First, lipophilicity may favor the more lipophilic MeO group over an OH group. However, substitution at C(3) with a long, lipophilic, aliphatic chain decreases activity (**31**). Second, the OH group in position 3(6) is much more acidic than in other positions, leading to a greater proportion of ionized form present at physiological pH. This is due to the OH group in position 3(6) of xanthones being located *para* to the C=O function. This property is used to characterize 3(6)-

Table 1. *MAO Inhibitory Activities of Xanthone Derivatives*

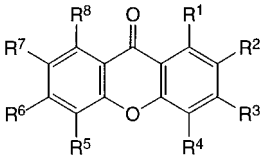

									IC_{50} [μM]	
No.	R^1	R^2	R^3	R^4	R^5	R^6	R^7	R^8	MAO-A	MAO-B
1[a][b]	H	H	H	H	H	H	H	H	0.84 ± 0.08	122 ± 14
2[a][b]	OH	H	H	H	H	H	H	H	0.31 ± 0.05	15 ± 1.9
3[a][b]	MeO	H	H	H	H	H	H	H	0.9 ± 0.1	33% (150 μM)
4[a][b]	H	OH	H	H	H	H	H	H	3.8 ± 0.3	23 ± 2.0
5[a][b]	H	MeO	H	H	H	H	H	H	5.3 ± 0.4	25 ± 4.7
6[a][b]	H	H	OH	H	H	H	H	H	1.1 ± 0.3	41 ± 9.2
7[a][b]	H	H	MeO	H	H	H	H	H	0.18 ± 0.03	7.6 ± 0.6
8[a][b]	H	H	H	OH	H	H	H	H	1.3 ± 0.1	155 ± 7
9[a][b]	H	H	H	MeO	H	H	H	H	30 ± 3.2	inact. (50 μM)
10[a][b]	OH	H	H	H	OH	H	H	H	0.73 ± 0.1	76 ± 9.4
11[a][d]	H	H	OH	H	OH	H	H	H	4.5 ± 0.2	30% (100 μM)
12[a][b]	H	H	OH	H	MeO	H	H	H	23 ± 1.4	119 ± 5.3
13[a][b]	OH	H	MeO	H	H	H	H	H	0.11 ± 0.01	0.86 ± 0.03
14[a][b]	MeO	H	MeO	H	H	H	H	H	20.2 ± 0.48	26% (20 μM)
15[a][b]	H	H	MeO	H	MeO	H	H	H	36 ± 2.9	71 ± 2.1
16[a][d]	MeO	H	H	H	OH	H	H	H	51 ± 7.8	123 ± 14
17[a][b]	H	H	MeO	OH	H	H	H	H	18 ± 3.1	37 ± 7.0
18[a][b]	H	H	OH	MeO	H	H	H	H	65 ± 6.8	90 ± 12
19[a][b]	H	H	MeO	MeO	H	H	H	H	31 ± 4.8	41 ± 7.7
20[b]	H	MeO	MeO	MeO	H	H	H	H	10% (30 μM)	27% (30 μM)
21[a][c]	OH	H	OH	H	OH	H	H	H	3.8 ± 0.25	73 ± 11
22[a][e]	OH	H	MeO	H	OH	H	H	H	0.04 ± 0.005	33 ± 5.5
23[a][e]	OH	H	MeO	H	MeO	H	H	H	29 ± 4.3	28% (30 μM)
24[a][b]	MeO	H	MeO	H	MeO	H	H	H	58 ± 6.8	34 ± 2.2
25[b]	OH	H	OH	Me	H	H	H	H	4.3 ± 0.4	16% (50 μM)
26[b]	OH	Me	OH	H	H	H	H	H	3.7 ± 0.2	22% (50 μM)
27[b]	OH	Me	OH	Cl	H	H	H	H	27 ± 1.1	inact. (100 μM)
28[b]	OH	Me	OH	Br	H	H	H	H	14.9 ± 0.6	inact. (150 μM)
29[f]	OH	H	OH	$C_{10}H_{17}$	OH	H	H	H	37 ± 5.5	66 ± 9.1
30[g]	OH	C_5H_9	H	OH	OH	H	H	H	3.3 ± 0.2	10% (30 μM)
31[f][h]	OH	H	C_5H_9	OH	OH	H	H	H	40 ± 3.7	32% (40 μM)
32[f][h]	OCH_3	H	C_5H_9	MeO	MeO	H	H	H	18% (40 μM)	9% (40 μM)
33[a][i]	OH	MeO	OH	H	OH	H	H	H	2.7 ± 0.4	68 ± 9.8
34[a][i]	OH	MeO	OH	H	MeO	H	H	H	51 ± 11	72 ± 8.3
35[j]	OH	MeO	MeO	H	OH	H	H	H	40% (40 μM)	14% (40 μM)
36[k]	OH	MeO	MeO	H	MeO	H	H	H	31% (25 μM)	24% (25 μM)
37[a][c]	MeO	MeO	MeO	H	MeO	H	H	H	37 ± 2.0	60 ± 12
38[a][e]	OH	H	OH	H	H	H	OH	H	8 ± 1.2	61 ± 9.8
39[a][m]	OH	H	OH	H	OH	H	H	OH	13 ± 1.4	0% (25 μM)
40[a][m]	OH	H	MeO	H	OH	H	H	OH	0.66 ± 0.06	9% (20 μM)
41[c]	MeO	H	MeO	H	MeO	H	H	MeO	22% (25 μM)	32% (25 μM)
42[a][e]	OH	H	OH	H	H	H	OH	OH	24 ± 4.6	25 ± 1.5
43[a][e]	OH	H	MeO	H	H	H	OH	OH	8.5 ± 0.8	5.7 ± 0.8
44[e]	Oprim[l])	H	MeO	H	H	H	OH	OH	48 ± 10	49 ± 12
45[a][e]	OH	H	MeO	H	H	H	MeO	MeO	19 ± 1.0	14.7 ± 0.90

Table 1 (cont.)

No.	R^1	R^2	R^3	R^4	R^5	R^6	R^7	R^8	IC_{50} [μM] MAO-A	IC_{50} [μM] MAO-B
46[a][c]	OH	H	OH	H	H	OH	OH	H	25 ± 3.4	90 ± 20
47[e]	OH	H	MeO	H	MeO	OH	MeO	OH	36% (75 μM)	22% (75 μM)
48[e]	OH	H	MeO	H	MeO	OH	MeO	MeO	27% (100 μM)	30% (100 μM)
49[e]	OH	H	MeO	H	MeO	MeO	MeO	OH	11% (15 μM)	18% (15 μM)
50[n]	MeO	H	H	Me	OH	H	MeO	H	24 ± 7.0	27% (50 μM)
51[o]	OH	H	MeO	MeO	H	H	OH	H	33% (50 μM)	17% (50 μM)
52[p]	OH	Glc	OH	H	H	OH	OH	H	87 ± 10	112 ± 14
53[a][i]	OH	MeO	OH	H	MeO	OH	H	H	32 ± 5.0	97 ± 14
54[d]	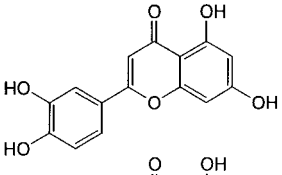								12 ± 2.1	38 ± 5.9
55[d]	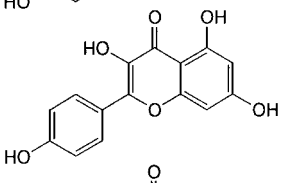								3.9 ± 0.4	48 ± 5.8
56[d]	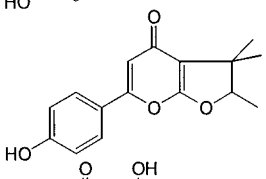								32 ± 1.5	6.7 ± 0.7
57[d]	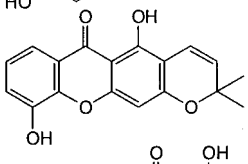								12 ± 1.1	47 ± 4.4
58[g]	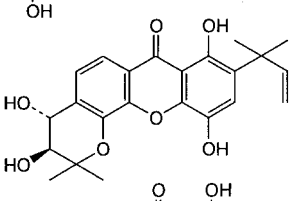								42% (100 μM)	31% (100 μM)
59[g]	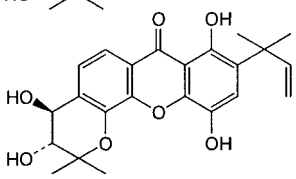								40% (100 μM)	30% (100 μM)

[a]) 34 Compounds in the training set. [b]) Synthetic compound. [c]) Partly synthetic compound. [d]) Isolated from *Hypericum brasiliense*. [e]) Isolated from *Chironia krebsii*. [f]) Isolated from *Garcinia livingstonei*; $C_{10}H_{17}$ is $Me_2C{=}CH{-}CH_2{-}CH_2{-}C(Me){=}CH{-}CH_2$. [g]) Isolated from *Garcinia gerrardii*; C_5H_9 is $CH_2{=}CH{-}CMe_2$. [h]) C_5H_9 is $Me_2C{=}CH{-}CH_2$. [i]) Isolated from *Monnina obtusifolia*. [j]) Isolated from *Monnina sylvatica*. [k]) Isolated from *Halenia campanulata*. [l]) Prim: primeverose. [m]) Isolated from *Gentiana lactea*. [n]) Isolated from *Pentadesma reyndersii*. [o]) Isolated from *Polygala virgata*. [p]) Isolated from *Eriosema tuberosum*.

hydroxyxanthones in UV spectroscopy, since adding a weak base such as NaOAc induces a bathochromic UV shift [11].

Substitution at C(2) does not significantly influence MAO-A inhibitory activity, as evidenced by comparing **4** with **5**, and **21** with **33**. Even a bulky substituent, as present in the prenylated compound **30**, did not affect MAO-A inhibitory activity. Mangiferin (**52**), the *C*-glycoside of **46**, was less active than its aglycone. Surprisingly, the relatively large glycosylated compounds **44** and **52** were still slightly active ($IC_{50} < 100$ μM) on both isozymes. This indicates that the active site of the two isoenzymes may be relatively flat and accessible. In contrast to compounds **58** and **59**, which have an additional ring connecting C(5) and C(6), a fourth ring connecting C(2) and C(3) does not appear to influence activity (**57**).

2.2. *Kinetics of Inhibition*. Extensive enzyme kinetic studies were carried out with compounds **22** and **25** selected for their activity. The *Lineweaver-Burk* plots of MAO-A inhibition by compound **22** (*Fig. 1*) and **25** (not shown) indicated a competitive mechanism of inhibition.

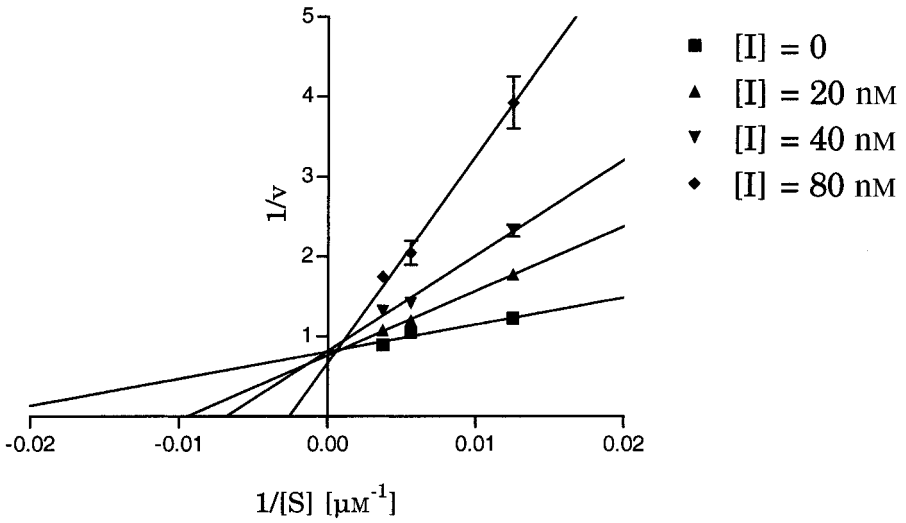

Fig. 1. Lineweaver-Burk *plot for MAO-A inhibition by compound* **22**

The inhibition by some MAO inhibitors, *e.g.*, moclobemide, has been shown to be influenced by the duration of preincubation. Preincubating the xanthones for 5 or 15 min at IC_{50} at the same substrate concentration made no difference in the degree of inhibition (results not shown). Thus, all xanthones appear to act on MAO by a reversible and probably competitive mechanism.

2.3. *Electronic Absorption Spectroscopy. Fig. 2* compares the electronic absorption spectra of solutions containing a constant lumiflavine concentration and various concentrations of inhibitor. The results for the equilibrium constants for the molecular complexation of the three tested compounds measured at 6, 13, 23, and 36°, are presented in *Table 2*.

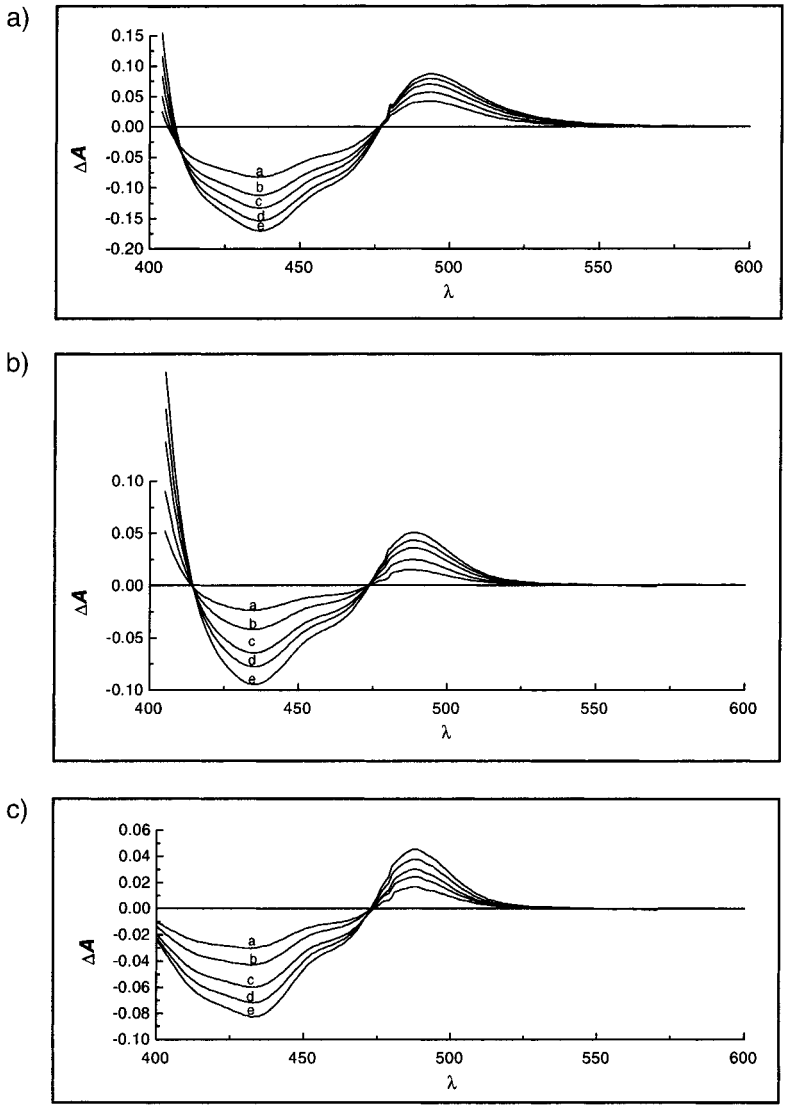

Fig. 2. *Difference absorption spectra at 13° of lumiflavine* (10^{-4} м) *with* a) *harmane at 1 m*м (a), *1.5 m*м (b), *2 m*м (c), *2.5 m*м (d), *3 m*м (e); b) *3-hydroxyxanthone* (**6**) *at 200* μм (a), *350* μм (b), *500* μм (c), *650* μм (d), *800* μм (e); c) *3-methoxyxanthone* (**7**) *at 150* μм (a), *225* μм (b), *300* μм (c), *375* μм (d), *450* μм (e)

The difference spectra show negative and positive bands. Since some amount of lumiflavine is involved in complex formation, the concentration of free lumiflavine in the sample cell is lower than in the reference cell, resulting in the negative peak at around 435 nm. Thus, the more negative the absorbance, the greater is the extent of complexation. The positive band corresponds to the charge-transfer transition (extra bands), characterizing the intermolecular complexation. This intermolecular complexation can be considered the first step in transfering an electron to the acceptor

Table 2. *Equilibrium Constants for the Complexation of the Tested Compounds with Lumiflavine Obtained from Absorption Spectroscopy Data*

No.	λ_{max} [nm]	K_D^{AC} [l/mol][a])			
		6°	13°	23°	36°
6	488	429 ± 58	305 ± 85	229 ± 30	41 ± 5
7	488	690 ± 82	533 ± 49	274 ± 18	227 ± 46
Harmane	492	383 ± 14	308 ± 14	218 ± 4	138 ± 10
Harmane[b])	492	548 ± 29[c])	414 ± 11[d])	314 ± 18[e])	220 ± 20[f])

[a]) Measurements in triplicate. [b]) Data taken from [26]. [c]) 5°. [d]) 15°. [e]) 27°. [f]) 45°.

lumiflavine. Thus, an examination of the difference spectra demonstrates the formation of a complex between a donor (harmane, **6**, or **7**) and the acceptor lumiflavine. The presence of isobestic points indicates a single complex of unitary stoichiometry.

2.4. *3D-QSAR According to the CoMFA/GOLPE Procedure.* The statistical results for the 34 molecules in the MAO-A training set are summarized in *Table 3*, which shows SAMPLS results before variable selection, and the final PLS coefficient values on the retained variables. The graphical results are shown in *Fig. 3*. The color code used to characterize the signals of each field is the following: favorable and unfavorable steric interactions are represented by green and red zones, respectively. Due to the duality of the electrostatic field, a white zone can mean a favorable influence of electron deficiency or an unfavorable influence of high electron density. The best model was obtained with the combination of steric and electrostatic (MEP, basis set STO-3G) fields. Lipophilicity was not retained as a relevant parameter to explain inhibitory activity.

A graphical representation of the model incorporating compounds **40** and **42** (*Fig. 3*) shows that a MeO group at C(3) is favorable for MAO-A inhibition, but that the same group at C(5) and C(7) is unfavorable. There is no signal around position 1. The electrostatic field reveals two zones, a magenta zone between positions 4 and 5 indicating the importance of an electron-rich zone, the density of which can vary depending upon the substitutions on the xanthone ring. The white zone around position 7 indicates a negative effect on activity of a MeO or OH group.

The structural difference between OH and MeO groups cannot be adequately revealed by a standard electrostastic field such as a Coulombic potential calculated from partial atomic charges. In fact, because the substituents are certainly influenced by the electronic properties of the xanthone ring, this structural complexity should be described by molecular electrostatic potentials (MEPs), explaining why the MEP was used instead of a standard electrostatic field.

2.5. *ALMOND Procedure.* The number of variables retained to build the final PLS model was 149 after one FFD application as described in the *Exper. Part*. The final model was built with four latent variables and cross-validated with the leave-one-out procedure ($q^2 = 0.66$, $r^2 = 0.86$).

The PLS coefficient histogram on *Fig. 4* shows only the most important pairs of nodes explaining MAO-A inhibitory activity (CC, NN, CN, and ON) and the distance separating each pair of nodes, which is about half the value indicated for each interaction type. NN Interaction energies can have either a positive effect on activity, at

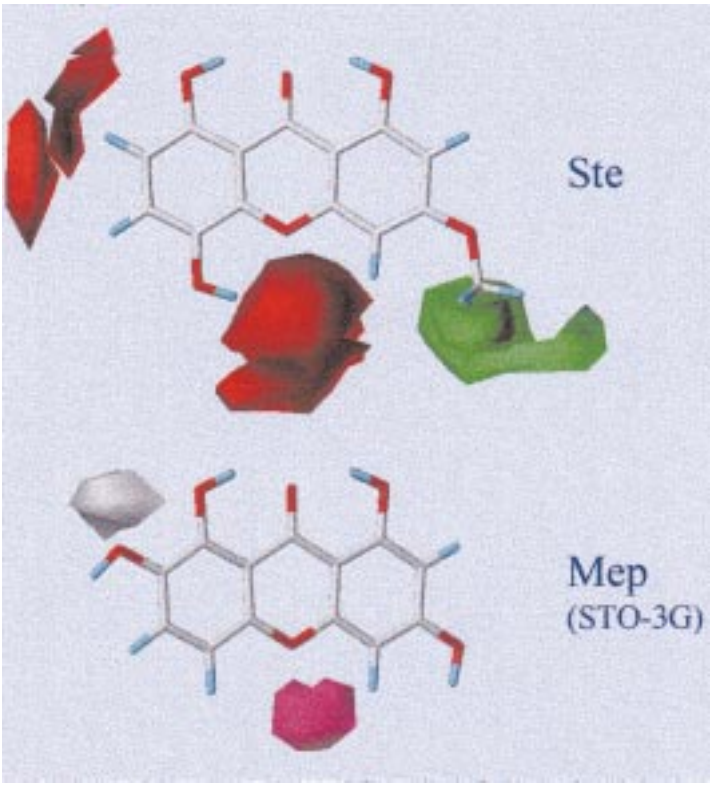

Fig. 3. *CoMFA/GOLPE Graphical results of the final PLS analysis of MAO-A inhibitors: representation of the statistical fields* (PLS coefficients) *obtained after variable selection in GOLPE*. The color codes: sterically favorable and non-favorable influences, green and red zones, respectively; favorable influence of high electron density and deficiency, magenta and white zones, respectively.

Table 3. *Statistical Results for CoMFA with a Data Set of 34 MAO-A Inhibitors*

	Variables	*N*	Fields	q^2	r^2
SAMPLES	4752	3	Ste + Mep	0.64	–
Final PLS[a])	859	3	Ste + Mep	0.74	0.87

[a]) The variables were selected with the fractional factorial design procedure after an advanced pretreatment.

the distance indicated by value 18, namely 9 Å, or a negative effect at a longer distance of 14.5 Å. The same is true for CN and ON interaction energies. Concerning CC interaction energies at short distances, the major effect is unfavorable for activity. These considerations can be illustrated by representing the vectors corresponding to the distances between the nodes. *Fig. 5* illustrates four cases, two of them revealing active compounds (*a* and *b*) and the others (*c* and *d*), poorly active compounds. CO Interactions at short distances (a) are positive for activity and show the importance of a free space between positions 4 and 5, generating more intense field-field interactions.

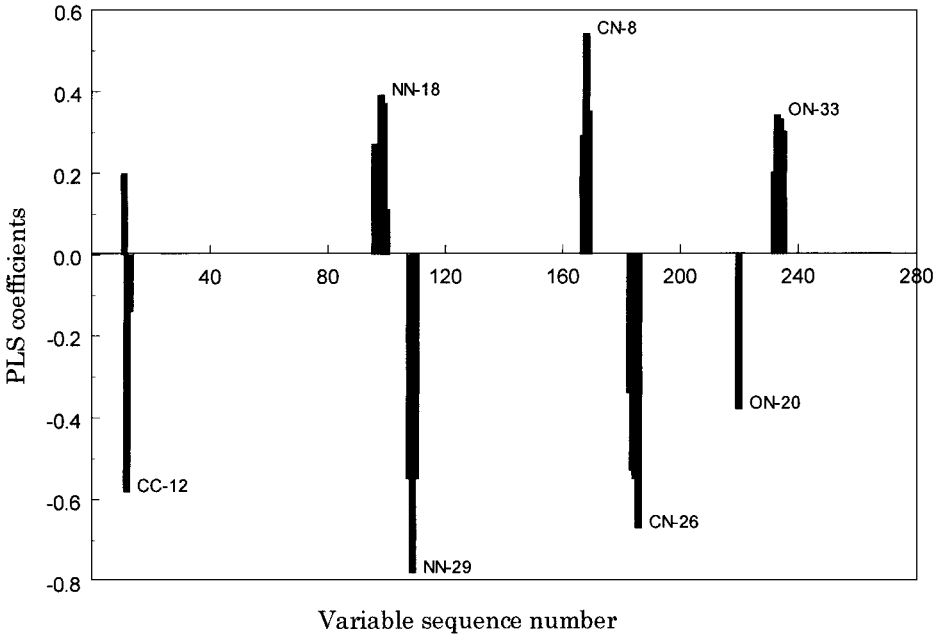

Fig. 4. *PLS Coefficients histogram illustrating the final PLS analysis after variable selection* (PC 4). The most important interactions are revealed by the Me (CC) and amide (NN) probes, and by the combinations methyl/amide (CN) and carbonyl/amide (ON). The positive and negative coefficients indicate a favorable or an unfavorable effect of the field-field interaction on activity.

The same kind of interaction at a longer distance (*Fig. 5*, *d*) is unfavorable for activity. In this case, the presence of an OH group in the symmetrical positions 3 or 6 decreases activity (compare **21** to **10**, **11** to **8**, and **19** to **9**). NN Interaction energies are favorable at relatively short distances as illustrated in *Fig. 5*, *b*, with the most active compound (**22**). The presence of an H-bond donor group in position 1 or 8 is a positive requirement for activity (compare **2** to **1**, and **10** to **8**). In the case of NN interactions at a longer distance, *Fig. 5*, *c*, reveals that the presence of an H-bond acceptor group in position 5 or 4 decreases activity.

2.6. *Cluster Analysis. Table 4* shows the field-field energy products retrieved for the data set of xanthone derivatives. The compounds are listed in the same order as classified by the dendrogram (not shown). This allows a general view of which vectors are present in each compound, and if their influence on activity is positive (+) or negative (−). The compounds are distributed in a bimodal way. In fact, two large clusters of approximately the same size (*A* and *B*) were generated. Cluster A contains molecules substituted with groups that cannot form H-bonds (MeO and H), or which contain a 1-OH substituent able to create an intramolecular H-bond with the C=O group of the xanthone ring. However, compounds **8**, **10**, and **22** belong to cluster *A*, and they are substituted with an OH group at C(4) or C(5). It is interesting to note that, for these three compounds, there is also the possibility of intramolecular H-bond formation. In consequence, the common features of compounds belonging to cluster

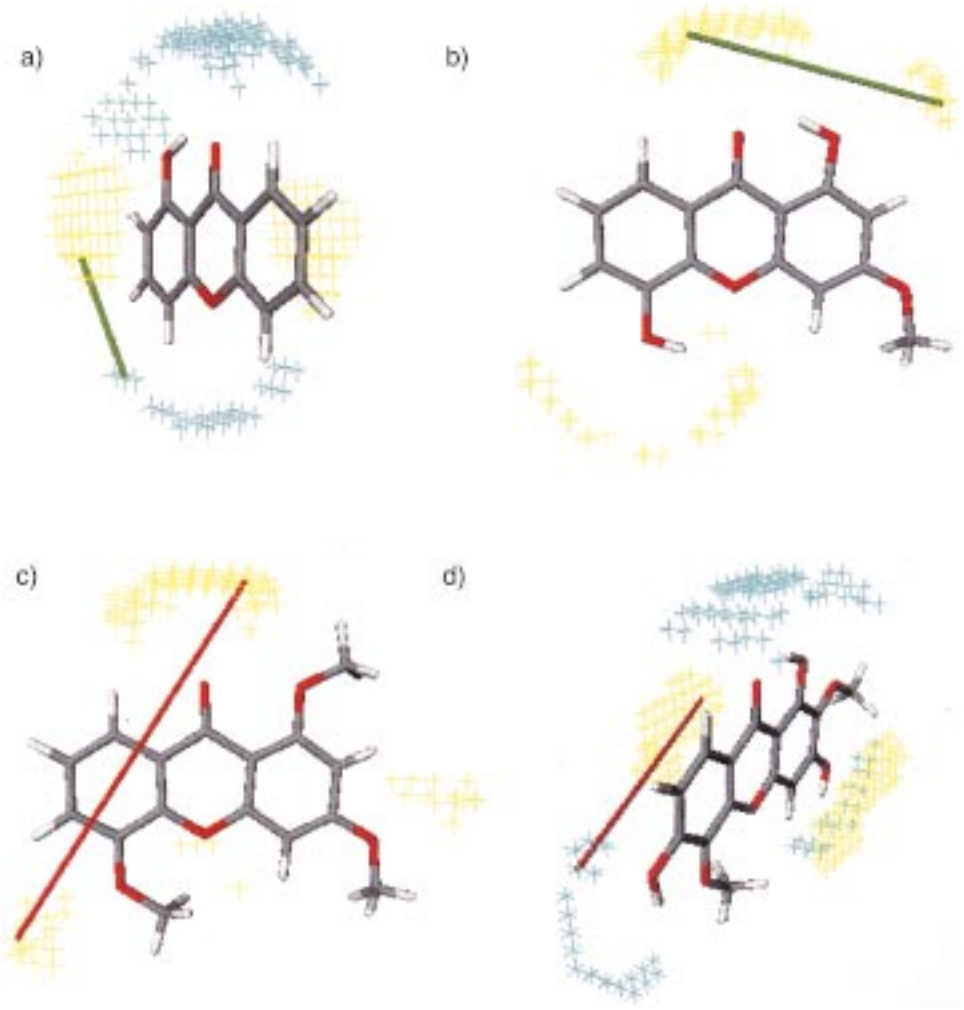

Fig. 5. *Illustration of some vectors important for MAO-A activity.* (+) and (−) for favorable and unfavorable to activity, respectively. *a*) Vector carbonyl-amide CN-8 (4 Å, +) present in compound **2**. *b*) Vector amide-amide NN-18 (9 Å, +) in compound **22**. *c*) Vector amide-amide NN-29 (14.5 Å, −) in compound **24**. *d*) Vector carbonyl-amide CN-26 (13 Å, −) in compound **53**.

B is that they possess a 'free' OH substituent. Looking at the smaller clusters as shown in *Table 4*, we can see that, globally, the molecules belonging to the same range of activity are described by the same kinds of field-field interactions. In summary, the most active compounds all have a favorable CN and NN interaction energies, while the NN interactions at long distances decrease activity.

3. Conclusion. – Members of a series of natural and synthetic xanthones are shown here to be competitive, reversible MAO-A inhibitors. The activities of the xanthone

Table 4. *Classification of the MAO-A Inhibitors Following Cluster Analysis.* Energy products of the interactions between the corresponding probes at the distance specified. The sequence of the compounds is related to their relative position in the dendrogram. *A* and *B* represent the two largest clusters.

No.	Products of the associated field energies[a])[b])[c])							
	pIC_{50}	CN-8 (+)	NN-18 (+)	ON-33 (+)	NN-29 (−)	CN-26 (−)	CC-12 (−)	ON-20 (−)
A								
1	6.08	0.40						0.16
5	5.28	0.42						0.16
8	5.90	0.43			0.65			0.36
17	4.74	0.45			0.61		0.38	0.35
2	6.51	0.42	0.65					0.16
13	6.96	0.44	0.71					0.17
3	6.03	0.49	0.47					0.17
7	6.74	0.42	0.54					0.17
9	4.52		0.52		0.53			0.17
19	4.51	0.44	0.54		0.50			0.18
23	4.55	0.44	0.64		0.51			0.18
15	4.44	0.43	0.54		0.53	0.40		0.18
10	6.14	0.52	0.64	0.53	0.61			
22	7.40	0.46	0.64	0.53	0.60			
14	4.70	0.48	0.51		0.44	0.40	0.38	0.17
24	4.24	0.44	0.52		0.54	0.42	0.43	0.18
37	4.43	0.51	0.55		0.54	0.43	0.51	0.19
45	4.72	0.52	0.68		0.48		0.46	0.17
B								
4	5.42	0.40	0.65		0.56	0.41		0.64
6	5.94	0.40	0.61		0.65	0.43		0.61
18	4.19		0.61		0.64	0.42		0.61
12	4.64		0.60	0.33	0.65	0.48		0.61
21	5.42		0.64	0.57	0.64	0.44		0.56
33	5.58		0.66	0.53	0.60	0.49		0.53
38	5.08		0.64	0.63	0.64	0.50		0.68
16	4.30		0.75		0.66	0.48	0.41	0.37
34	4.29		0.66	0.27	0.59	0.48	0.45	0.35
39	4.87		0.64	0.61	0.62	0.51	0.43	0.67
53	4.49		0.65	0.59	0.62	0.54	0.46	0.66
42	4.63		0.64	0.62	0.61	0.50	0.44	0.62
46	4.60		0.64	0.61	0.63	0.49	0.41	0.74
11	5.35	0.45	0.60	0.55	0.64	0.44		0.61
43	5.07	0.44	0.64	0.53	0.58	0.52	0.45	0.53
40	6.18	0.47	0.64	0.56	0.60		0.44	0.50

[a]) Field values were normalized between 0 and 1 by dividing the value of the energy of interaction by a constant representing a theoretical maximum of energy for a specific probe. Therefore, their products vary between 0 and 1. [b]) The distance between the interacting nodes is about half the value of that indicated after the interaction type. [c]) (+)- or (−): positive or negative influence of the vector on activity, respectively (*cf. Fig. 4*). Blanks indicate that the vector considered was not present for the corresponding compound.

series are comparable to some reported inhibitors (*e.g.*, a nitrogen-free tricyclic series with inhibitor activities ranging from 40 nM to 30 μM [11]), with compound **22** emerging as one of the most potent MAO-A inhibitors of natural origin. However, it is not as active and selective as the synthetic MAO-A inhibitors befloxatone ($K_i = 2.3$ nM) and cimoxatone ($K_i = 1$ nM) [12].

The molecular mechanism by which these compounds inhibit monoamine oxidase remains poorly understood. A possible mechanism involves charge-transfer interaction with the FAD cofactor, as documented for harmine, brofaromine, and toloxatone [13]. Electron-absorption spectroscopy studies indicate that xanthone derivatives act *via* a charge-transfer mechanism with the FAD cofactor of MAO-A. In fact, there was formation of a complex between the three donors tested (harmane, and compounds **6** and **7**) and the acceptor lumiflavine.

SAR Studies revealed the importance of an OH substituent in position 1(8) or 5 instead of an MeO substituent. The contrary is true for position 3, where MeO substituents lead to more active compounds than OH substituents. CoMFA/GOLPE yielded additional information regarding the importance of an electron-rich zone between positions 4 and 5, and the unfavorable effect of an electron-rich zone around position 7. However, the statistical treatment of this apparently simple series is not easy due to its limited structural variability. This problem is reinforced in the case of xanthone derivatives, because the electronic nature of the ring is complex and probably plays a role in the inhibition mechanism.

The ALMOND approach proved interesting, first to avoid alignment problems due to the symmetry of the xanthone ring, and also because it generates novel descriptors to explain MAO-A inhibitory activity. This study revealed the importance of the distance between two H-bond-acceptor groups (with NN interaction energies) in modulating activity. The same is true for the interaction between the methyl and amide probes (CN). Due to the relatively high number of substituted positions on the xanthone ring, it must be kept in mind that the activity of a compound is governed by the combined effects of all substituents. If a compound contains a vector favorable to activity and two unfavorable ones, the global effect can be negative or positive depending on the intensity of the field-field interactions.

The promising MAO inhibitory activities reported here remain to be confirmed in *in vivo* experiments. Since herbal medicines are currently receiving much attention, it will also be interesting to test active plant extracts *in vivo*.

Xanthones of natural and synthetic origin are not only interesting for the design of new antidepressant drugs, but also because they interfere with the toxification mechanism involving radical formation. By inhibiting MAO-B and MAO-A, the formation of H_2O_2 could be decreased. A second mode of action of hydroxylated xanthones could be iron-ion chelation, as already described for flavonoids [14].

B. Testa and *P.-A. Carrupt* are indebted to the *Swiss National Science Foundation* for support.

Experimental Part

Computations. All calculations were run on *Silicon Graphics Indy R4400* 175 MHz and *Origin 2000 4R10000* 195 MHz workstations with the *SYBYL 6.6* molecular modeling package (*Tripos Associates*, St. Louis, MO, USA). Minimal-energy conformations were obtained with the *MMFF94s* force field [15]. Molecular Electrostatic Potentials (MEPs) were calculated with Gaussian 98 [16] software and the STO-3G basis set. The

Molecular Lipophilicity Potential (MLP) was used as a third field [17]. The other computational tools used were ALMOND [18], GRID version 1.7 [19], GOLPE [20], and TSAR 3.0 [21].

Inhibitory Activities. The method of *Weissbach et al.* [22] was modified to measure inhibitory activities [23]. Kynuramine, a non-selective MAO substrate, was used to measure enzymic activity. Kynuramine is deaminated by MAO to an aldehyde that spontaneously cyclizes to 4-hydroxyquinoline. Formation of this product was monitored spectrophotometrically at 314 nm with a *Kontron UVIKON 941* spectrophotometer. Deprenyl and clorgyline, two selective MAO-B and MAO-A irreversible inhibitors, were used to measure MAO-A or MAO-B activity, respectively.

Soluble compounds were tested in mitochondrial suspension/DMSO 95 : 5, up to a concentration of 150 μM. If no inhibitory effect was seen at 150 μM, the compound was defined as inactive. To measure IC_{50} values, incubations were carried out in duplicate with at least five concentrations of inhibitor ranging from 0.5 times to 16 times the previously estimated IC_{50} value [24]. The IC_{50} value was calculated by a hyperbolic function [25] and then verified in a separate experiment monitoring the formation of product and the disappearance of substrate at 360 nm. To validate the method, harmane was used as a standard inhibitor (MAO-A: IC_{50} 0.6 μM; MAO-B: IC_{50} 119 μM), in good agreement with literature data ([26]: MAO-A: IC_{50} 0.5 μM; MAO-B: IC_{50} 80 μM).

Reversibility was evaluated either by displacement or by dilution [27]. In the former procedure, inhibitory activities were measured at the IC_{50}, adding the substrate at a concentration of 5 times the K_M. With partial reversal of inhibition, the type of inhibition is not an uncompetitive one but, in all cases, a reversible one (competitive, non-competitive, and mixed inhibition). In the dilution procedure, mitochondrial samples were incubated with the inhibitors or with an equal volume of buffer at 37° for 30 min. The samples were then diluted 10-fold with the buffer soln. The inhibitor was then added at the IC_{50} in the assay mixtures containing only the buffer, so that the final concentration of inhibitor was the same in the assay mixture incubated either in the absence or in the presence of inhibitor. Finally, the substrate was added, and the samples were assayed by the method described above. For a reversible inhibitor, the degree of inhibition is the same with or without preincubation. With irreversible inhibitor, a greater degree of inhibition is observed following preincubation. Time dependence was tested for all inhibitors by comparing preincubations of 5 and 15 min.

Electron Absorption Spectroscopy. Charge-transfer complexation for compounds **6**, **7**, and harmane (a potent and very selective MAO-A inhibitor) was determined by electron-absorption spectroscopy. In solution, the interactions between a donor (D) and an acceptor (A) alter their absorption spectra and generate new transitions. These may be assigned to intermolecular charge transfer of the complex and occur at longer wavelengths than those of non-complexed molecules. As already described in [13], the interaction between D and A leads to the formation of an equilibrium between the non-complexed species and the charge transfer complex (*Eqn. 1*); the resulting thermodynamic complexation constant is defined by *Eqn. 2:*

$$D + A \rightleftharpoons AD \tag{1}$$

$$K_C^{AD} = \frac{[AD]}{[A][D]} \tag{2}$$

When there is formation of only one complex of stoichiometry 1 : 1, this constant can be written as:

$$K_C^{AD} = \frac{[AD]}{([A]_0 - [AD]) \cdot ([D]_0 - [AD])} \tag{3}$$

where $[A]_0$ and $[D]_0$ are the initial concentrations of the acceptor and donor, resp.

If only the formed complex absorbs at the wavelengths λ characteristic of the charge transfer, and if the initial concentration of the donor is greater than that of the acceptor, the *Foster-Hammick-Wardley* equation may be modified to yield the *Benesi-Hildebrand* equation:

$$\frac{A}{[D]_0} = -K_C^{AD} A + K_C^{AD} [D]_0 \varepsilon^{AD} \tag{4}$$

where A is the absorbance at the wavelength λ of the complex and ε its molar extinction coefficient in mol^{-1} cm^{-1}. For a series of solutions with D at different concentrations and A at a constant concentration, a plot of $A/[D]_0$ *vs.* A should be linear if $[D]_0 \gg [A]_0$. K_C^{AD} can then be calculated from the slope of the linear regression.

Lumiflavine was dissolved in a 0.15M phosphate buffer of pH 6.0 (Na_2HPO_4/K_2HPO_4) to a final concentration of 10^{-4} M. The MAO-A inhibitors under study were dissolved in DMSO (final concentration of 20% (*v*/*v*)) and added to the soln. of lumiflavine. The soln. was then incubated for 5 min at various temp. (between 6 and 36°). The differences in electron absorption were monitored between 385 and 650 nm with a

Kontron UVIKON 941 spectrophotometer in order to determine the K_C^{AD} value of complexation. The method was validated with harmane, which had already been shown to form a charge-transfer complex with riboflavine [28].

CoMFA/GOLPE Procedure. The training set consisted in 34 compounds (*Table 1*), where structural variability was restricted to three types of substituents, namely H, OH, and MeO groups in the 8 positions of the xanthone ring. The superposition of compounds studied in a biologically relevant conformation is a critical step in any CoMFA study. Here, the most obvious alignment is the superposition of the xanthone ring system. Nevertheless, two points were examined: *1*) Since the xanthone ring system is symmetric, compounds **8** and **9**, for example, could be inverted to have their 4-substituent corresponding to the 5-position of other xanthones. Depending on the activity of the compounds, the orientation chosen corresponded to that of compounds with a similar potency. *2*) The OH and MeO groups were kept in the plane of the xanthone ring. This orientation is a stable one and allows possible H-bonds between two adjacent positions. In positions 1 and 4 the H-atom was oriented to form an intramolecular H-bond with the C=O group of the xanthone ring, while, in positions 5 and 8, it was directed toward the ether group. For the other positions, the H-atom was orientated to form always a H-bond with the successive position.

The CoMFA region was defined by a grid of 1.0 Å. First, SAMPLS analysis was carried out in SYBYL to determine which fields or combination thereof were the most important for activity. Inhibitory activities were expressed as pIC_{50} values. The retained molecular fields were then exported in GOLPE, which offers more useful tools. A principal component analysis (PCA) was then applied in order to observe the repartition of the objects in the space of the three first principal components (PCs). An advanced pretreatment was performed on the steric (ste) and electrostatic (mep) fields. 'Zeroing' positive and negative values was applied (ste: $+0.5/-0.1$; mep: $+0.5/-0.1$ kcal/mol), as well as a standard deviation cutoff (ste: 0.1; mep 1.0 kcal/mol). The 2-, 3-, and 4-level variables were removed, and the weights were set in order to give the same importance to each field. A grouping of variables was then applied by means of the Smart Region Definition (SRD) algorithm: 475 seeds selected on PLS weights space, critical distance cutoff of 1.0 Å, and collapsing distance cutoff of 2.0 Å. A variable selection was then applied by means of the Fractional Factorial Design (FFD) algorithm. The groups of variables were used with a 5:1 ratio of true/dummy variables and a 2:1 ratio of combinations/variables. The cross-validation mode chosen was 'random groups' with five groups, and the weights were recalculated after object exclusion. Noisy variables were excluded, and the uncertain ones were retained. The graphical results represent the most relevant regions of space where the variations of the statistical field (PLS coefficient) were the largest.

ALMOND Procedure. Alignment is a critical step in any CoMFA study. The structures studied in the present work have a symmetric ring system alignment of which, in a CoMFA study, can strongly influence the final result. To avoid any bias, we used an additional approach to complete the CoMFA study and submitted the same training set of MAO-A inhibitors to the ALMOND procedure. The descriptors generated are independent of alignment and are called GRid Independent Descriptors (GRIND). They are the result of the transformation of a Molecular Field Interaction (MIF) generated with the GRID program. To obtain an accurate picture of the ability of a ligand to interact with a receptor, a certain number of MIFs obtained with different probes are required.

MIFs were obtained with the GRID program, and GRIND were generated, analyzed, and interpreted by means of the program ALMOND. The three probes used were methyl (C), carbonyl (O), and amide (N) in order to represent steric, H-bond-donor, and H-bond-acceptor interactions with a virtual receptor site (VRS). OH Groups in position 1 and/or 8 were kept fixed when computing the MIFs, because of possible intramolecular H-bond formation. Otherwise, free rotation of substituents was maintained. The MIFs so generated were filtered by extracting from the grid fields, for each object, a reduced subset of informative positions or nodes. A grid spacing of 0.5 Å was used, and 100 nodes were extracted with 35% field weight. The aim is to try to represent the independent pharmacophoric groups by which the ligand can interact. The algorithm used selects from each MIF a fixed number of nodes optimizing a scoring function including two criteria: the intensity of a field at a node and the node-node distance between the chosen nodes. Consequently, favorable probe-ligand interaction regions are extracted. These regions define the VRS. Then, a MACC (Maximum Auto and Cross Covariance) transform method was used, in which only the maximum value of the products of the two i and j field values, found at each different r_{ij} distance, are represented in the auto-correlograms. Only the maximum value was stored for each distance, and the spatial position of the nodes generating this interaction was also stored. For each set of MIFs considered, the MACC transform computes the auto-correlograms and the corresponding cross-correlograms, *e.g.*, in the case of two MIFs N and O, the MACC transform will compute the auto-correlograms NN and OO, and the cross-correlogram NO.

To build the final model, a FFD variable selection procedure [29] was applied according to the following criteria: four latent variables, random group cross-validation procedure (five groups), and retaining uncertain variables. A PLS analysis was finally carried out on the remaining variables according to the classical 'leave-one-out' cross-validation procedure.

Cluster Analysis. To have a clearer view of the important features required for MAO-A inhibitory activity, a cluster analysis was carried out in TSAR 3.0. The same training set as the one submitted to CoMFA/GOLPE and ALMOND was used. For each compound, the value of each of the most important field-field interactions, as revealed by the final ALMOND PLS analysis (*Fig. 4*), was retrieved from the corresponding correlogram. Each of these values correspond to the energy product of a field-field interaction at a specific distance (NN, CN...,). These data were submitted to a cluster analysis, and a dendrogram was generated (not shown), which allowed us to classify the compounds in *Table 4*.

Compounds. The investigated xanthones and related compounds (*Table 1*) were isolated from *Chironia krebsii* (Gentianaceae) (**22**, **23**, **38**, **42**–**45**, **47**–**49**) [30], *Hypericum brasiliense* (Guttiferae) (**10**, **16**, **54**–**57**) [31], *Garcinia livingstonei* (Guttiferae) (**29**, **31**, **32**) [32][33], *Gentiana lactea* (Gentianaceae) (**39**, **40**) [34], *Garcinia gerrardii* HARVEY (Guttiferae) (**30**, **58**, **59**) [35], *Monnina obtusifolia* (Polygalaceae) (**33**, **34**, **53**), *Polygala virgata* (Polygalaceae) (**51**) [36], *Monnina sylvatica* (Polygalaceae) (**35**) [37], *Halenia campanulata* (Gentianaceae) (**36**), *Pentadesma reyndersii* (Guttiferae) (**50**), and *Eriosema tuberosum* (Leguminosae) (**52**) [38][39]. The syntheses of the other compounds have already been described according to the references cited below. Xanthone was purchased from *Fluka Chemie AG*, CH-Buchs.

Chemistry. Purification by column chromatography (CC) was carried out on *Merck* silica gel *60* (0.50–0.20 mm) and anal. TLC employing silica gel *GF 254 Merck* (type *60*). M.p.: *Kofler* microscope; uncorrected. IR Spectra: *Perkin-Elmer 257* or *ATI-Mattson Elmer 257*; KBr; only the most IR absorption bands are listed. NMR Spectra: at 300 MHz on a *Bruker AMX-300* instrument for ^{1}H and 75.47 MHz for ^{13}C in (D_6)DMSO (99.0%); chemical shifts are expresssed in δ (ppm), coupling constant J in Hz; Me_4Si as reference. MS: *Hitachi Perkin-Elmer RMU-6M* Spectrometer.

The following materials were synthesized and purified by the described procedures.

1-Hydroxyxanthone (**2**). Obtained according to the procedure described in [40]. ^{1}H-NMR ((D_6)DMSO): 12.56 (*s*, OH); 8.18 (*dd*, J = 8.2, 1.7, H–C(8)); 7.92 (*ddd*, J = 8.1, 7.6, 1.7, H–C(6)); 7.74 (*dd*, J = 8.3, 8.2, H–C(3)); 7.67 (*d*, J = 8.1, H–C(5)); 7.51 (*dd*, J = 8.2, 7.6, H–C(7)); 6.83 (*dd*, J = 8.3, 0.6, H–C(2)). ^{13}C-NMR ((D_6)DMSO): 181.8 (C(9)); 161.0 (C(1)); 155.8 (C(4a)); 155.7 (C(4b)); 137.6 (C(3)); 136.5 (C(6)); 125.5 (C(8)); 124.7 (C(7)); 119.9 (C(8a)); 118.1 (C(5)); 110.2 (C(2)); 108.4 (C(8b)); 107.3 (C(4)).

1-Methoxyxanthone (**3**). Obtained from **2** according to the procedure described in [41]. ^{1}H-NMR ((D_6)DMSO): 8.09 (*dd*, J = 7.7, 1.6, H–C(8)); 7.80 (*ddd*, J = 7.8, 7.6, 1.6, H–C(6)); 7.74 (*dd*, J = 8.4, 8.3, H–C(3)); 7.57 (*dd*, J = 7.8, 0.7, H–C(5)); 7.42 (*ddd*, J = 7.7, 7.6, 0.7, H–C(7)); 7.00 (*d*, J = 8.3, H–C(2)); 3.91 (*s*, MeO). ^{13}C-NMR ((D_6)DMSO): 174.7 (C(9)); 160.2 (C(1)); 157.4 (C(4a)); 154.4 (C(4b)); 135.7 (C(3)); 134.8 (C(6)); 125.9 (C(8)); 124.2 (C(7)); 122.4 (C(8a)); 117.5 (C(5)); 111.6 (C(8b)); 109.6 (C(4)); 106.4 (C(2)).

2-Methoxyxanthone (**5**). Obtained through a benzophenone intermediate according to the procedure described in [42]. M.p. 128–129° ([43]: 128–130°). IR (KBr): 1650, 1614, 1489, 1467, 1317, 1212, 1142, 1024, 761. ^{1}H-NMR ((D_6)DMSO): 8.18 (*dd*, J = 7.7, 1.7, H–C(8)); 7.86 (*ddd*, J = 8.2, 7.4, 1.7, H–C(6)); 7.64 (*dd*, J = 8.2, 1.9, H–C(5)); 7.63 (*d*, J = 9.1, H–C(4)); 7.54 (*d*, J = 3.2, H–C(1)); 7.47 (*dd*, J = 9.1, 3.2, H–C(3)); 7.46 (*ddd*, J = 7.7, 7.4, 1.0, H–C(7)); 3.87 (*s*, MeO). The ^{1}H-NMR data are in agreement with those given in [44]. ^{13}C-NMR ((D_6)DMSO): 175.8 (C(9)); 155.7 (C(2)); 155.5 (C(4b)); 150.3 (C(4a)); 135.4 (C(6)); 126.0 (C(8)); 124.7 (C(3)); 124.2 (C(7)); 121.5 (C(8b)); 120.5 (C(8a)); 119.8 (C(4)); 118.2 (C(5)); 105.7 (C(1)); 55.7 (MeO). The ^{13}C-NMR data are in agreement with those given in [45]. MS: 228 (2, $[M+2]^{+\cdot}$), 227 (16, $[M+1]^{+\cdot}$), 226 (100, $M^{+\cdot}$), 225 (27), 224 (3), 212 (6), 211 (36), 197 (13), 196 (19), 183 (6), 168 (4), 156 (3), 155 (26), 140 (1), 139 (8), 127 (20), 126 (7), 113 (10), 107 (6), 102 (1), 101 (7), 80 (5), 78 (8), 77 (5), 76 (8), 63 (15), 62 (5).

2-Hydroxyxanthone (**4**). Obtained by demethylation of **5** according to the procedure described in [42]. M.p. 202–205°. IR (KBr): 3220, 1615, 1600, 1481, 1462, 1341, 1232, 762. ^{1}H-NMR ((D_6)DMSO): 10.00 (*s*, OH); 8.19 (*dd*, J = 8.0, 1.7, H–C(8)); 7.85 (*ddd*, J = 8.2, 7.6, 1.7, H–C(6)); 7.63 (*dd*, J = 8.2, 0.9, H–C(5)); 7.56 (*d*, J = 9.0, H–C(4)); 7.48 (*d*, J = 3.0, H–C(1)); 7.45 (*ddd*, J = 8.0, 7.6, 0.9, H–C(7)); 7.32 (*dd*, J = 9.0, 3.0, H–C(3)). The ^{1}H-NMR data are in agreement with those given in [44]. ^{13}C-NMR ((D_6)DMSO): 175.9 (C(9)); 155.6 (C(4b)); 153.9 (C(2)); 149.2 (C(4a)); 135.2 (C(6)); 125.9 (C(8)); 124.6 (C(3)); 124.0 (C(7)); 121.7 (C(8b)); 120.4 (C(8a)); 119.5 (C(4)); 118.2 (C(5)); 108.5 (C(1)). The ^{13}C-NMR data are in agreement with those given in [46], except for C(8a) and C(8b) for which the chemical shifts are interchanged. MS: 214 (2, $[M+2]^{+\cdot}$), 213 (15, $[M+1]^{+\cdot}$), 212 (100, $M^{+\cdot}$), 184 (8), 155 (5), 128 (5), 127 (6), 106 (4), 92 (4).

3-Methoxyxanthone (**7**). Obtained by an alkaline cyclization of 2-hydroxy-2′,4-dimethoxybenzophenone according to the procedure described in [41]. M.p. 126–128° ([47]: 128–130°). IR (KBr): 1651, 1613, 1462, 1434, 1321, 1259, 1099, 1015, 829, 760. ^{1}H-NMR ((D$_6$)DMSO): 8.17 (*dd*, *J* = 7.7, 1.7, H–C(8)); 8.10 (*d*, *J* = 8.9, H–C(1)); 7.85 (*ddd*, *J* = 8.0, 7.6, 1.7, H–C(6)); 7.63 (*d*, *J* = 8.0, H–C(5)); 7.47 (*dd*, *J* = 7.7, 7.6, H–C(7)); 7.16 (*d*, *J* = 2.4, H–C(4)); 7.05 (*dd*, *J* = 8.9, 2.4, H–C(2)); 3.93 (*s*, MeO). The ^{1}H-NMR data are in agreement with those given in [39]. ^{13}C-NMR ((D$_6$)DMSO, 75.47 MHz): 174.9 (C(9)); 165.0 (C(3)); 157.6 (C(4a)); 155.6 (C(4b)); 135.1 (C(6)); 127.6 (C(1)); 125.9 (C(8)); 124.4 (C(7)); 121.2 (C(8a)); 117.9 (C(5)); 114.9 (C(8b)); 113.7 (C(2)); 100.6 (C(4)); 56.2 (MeO). The ^{13}C-NMR data are in agreement with those given in [48]. MS: 228 (2, $[M+2]^{+\bullet}$), 227 (19, $[M+1]^{+\bullet}$), 226 (100, $M^{+\bullet}$), 225 (7), 211 (1), 197 (11), 196 (6), 183 (18), 168 (8), 155 (12), 140 (1), 139 (6), 127 (10), 126 (4), 102 (1), 99 (4), 77 (4), 63 (11).

3-Hydroxyxanthone (**6**). Obtained by demethylation of (**7**) according to the procedure described in [44]. M.p. 194–197°. IR (KBr): 3130, 1617, 1568, 1483, 1455, 1316, 1160, 1114, 750. ^{1}H-NMR ((D$_6$)DMSO): 11.00 (*s*, OH); 8.15 (*dd*, *J* = 7.9, 1.7, H–C(8)); 8.04 (*d*, *J* = 8.6, H–C(1)); 7.82 (*ddd*, *J* = 8.2, 7.6, 1.7, H–C(6)); 7.61 (*d*, *J* = 8.2, H–C(5)); 7.44 (*dd*, *J* = 7.9, 7.6, H–C(7)); 6.91 (*dd*, *J* = 8.6, 2.2, H–C(2)); 6.88 (*d*, *J* = 2.2, H–C(4)). The ^{1}H-NMR data are in agreement with those given in [41]. ^{13}C-NMR ((D$_6$)DMSO): 174.8 (C(9)); 164.0 (C(3)); 157.6 (C(4a)); 155.6 (C(4b)); 134.9 (C(6)); 128.0 (C(1)); 125.9 (C(8)); 124.2 (C(7)); 121.2 (C(8a)); 117.9 (C(5)); 114.2 (C(2)); 114.0 (C(8b)); 102.1 (C(4)). The ^{13}C-NMR data are in agreement with those given in [46]. MS: 214 (2, $[M+2]^{+\bullet}$), 213 (16, $[M+1]^{+\bullet}$), 212 (100, $M^{+\bullet}$), 211 (6), 184 (14), 155 (6), 128 (7), 127 (5), 92 (14).

4-Methoxyxanthone (**9**). The 2-(2′-methoxyphenoxy)benzoic acid obtained initially by an *Ullman* reaction underwent an appropriate cyclization to **9** according to the procedure described in [49]. M.p. 173–176° ([50]: 174–175°). IR (KBr): 2929, 1660, 1601, 1497, 1468, 1448, 1340, 1280, 1232, 1075, 750. ^{1}H-NMR ((D$_6$)DMSO): 8.20 (*dd*, *J* = 8.0, 1.6, H–C(8)); 7.88 (*dt*, *J* = 8.1, 1.6, H–C(6)); 7.73 (*dd*, *J* = 7.9, 1.4, H–C(1)); 7.72 (*d*, *J* = 8.1, H–C(5)); 7.52 (*dd*, *J* = 7.9, 1.4, H–C(3)); 7.49 (*dd*, *J* = 8.0, 7.8, H–C(7)); 7.40 (*t*, *J* = 7.9, H–C(2)); 3.99 (*s*, MeO). ^{13}C-NMR ((D$_6$)DMSO): 176.0 (C(9)); 155.4 (C(4b)); 148.4 (C(4)); 145.8 (C(4a)); 135.5 (C(6)); 125.9 (C(8)); 124.5 (C(7)); 124.0 (C(2)); 121.0 (C(8a)); 121.9 (C(8b)); 118.4 (C(5)); 116.4 (C(3)); 116.4 (C(1)); 56.2 (MeO). MS: 228 (3, $[M+2]^{+\bullet}$), 227 (26, $[M+1]^{+\bullet}$), 226 (100, $M^{+\bullet}$), 212 (13), 211 (81), 183 (7), 168 (1), 157 (3), 156 (3), 155 (23), 140 (1), 139 (5), 127 (14), 126 (5), 113 (6), 107 (3), 102 (1), 101 (5), 77 (4), 76 (5), 63 (6), 58 (4), 51 (6).

4-Hydroxyxanthone (**8**). Obtained by demethylation of (**9**) according to the procedure described in [42]. M.p. 234–236° ([42]: 230–233°). IR (KBr): 3191, 1640, 1588, 1502, 1480, 1460, 1353, 1290, 1225, 1102, 1033, 753. ^{1}H-NMR ((D$_6$)DMSO): 10.51 (*s*, OH); 8.19 (*dd*, *J* = 7.8, 1.6, H–C(8)); 7.88 (*ddd*, *J* = 8.0, 7.6, 1.6, H–C(6)); 7.73 (*dd*, *J* = 8.0, 0.8, H–C(5)); 7.61 (*dd*, *J* = 7.8, 1.8, H–C(1)); 7.48 (*ddd*, *J* = 7.8, 7.6, 0.8, H–C(7)); 7.34 (*dd*, *J* = 7.8, 1.8, H–C(3)); 7.26 (*t*, *J* = 7.8, H–C(2)). ^{13}C-NMR ((D$_6$)DMSO): 176.2 (C(9)); 155.4 (C(4b)); 146.7 (C(4)); 145.2 (C(4a)); 135.4 (C(6)); 126.0 (C(8)); 124.3 (C(7)); 124.1 (C(2)); 122.2 (C(8b)); 120.9 (C(8a)); 120.2 (C(3)); 118.3 (C(5)); 115.2 (C(1)). The ^{13}C-NMR data are in agreement with those given in [46], except for C(2) and C(7) for which the chemical shifts are interchanged. MS: 214 (2, $[M+2]^{+\bullet}$), 213 (15, $[M+1]^{+\bullet}$), 212 (100, $M^{+\bullet}$), 211 (4), 184 (12), 155 (4), 128 (7), 127 (6), 106 (4), 102 (4), 92 (4), 83 (5), 64 (4), 63 (4), 59 (16).

3,5-Dihydroxyxanthone (**11**). Obtained through 2,2′,3′,4-tetramethoxybenzophenone [40][49][51] according to the procedure described in [52]. M.p. 274–275°. IR (KBr): 3356, 1643, 1581, 1489. ^{1}H-NMR ((D$_6$)DMSO): 8.02 (*d*, *J* = 9.4, H–C(1)); 7.56 (*dd*, *J* = 7.5, 1.8, H–C(8)); 7.27 (*dd*, *J* = 7.8, 1.8, H–C(6)); 7.21 (*t*, *J* = 7.7, H–C(7)); 6.89 (*dd*, *J* = 7.4, 2.1, H–C(2)); 6.88 (*s*, H–C(4)). ^{13}C-NMR ((D$_6$)DMSO): 175.0 (C=O); 163.9 (C(3)); 157.3 (C(4a)); 146.3 (C(5)); 145.8 (C(4b)); 127.9 (C(1)); 123.8 (C(7)); 122.0 (C(8a)); 116.1 (C(6)); 115.2 (C(8)); 114.2 (C(2)); 113.8 (C(8b)); 102.1 (C(4)).

3-Hydroxy-5-methoxyxanthone (**12**). Obtained through 2′,4-dihydroxy-2,3′-dimethoxybenzophenone [53] according to the procedure described in [43]. M.p. 315–317°. IR (KBr): 3078, 1580, 1500. ^{1}H-NMR ((D$_6$)DMSO): 8.03 (*d*, *J* = 8.6, H–C(1)); 7.7 (*dd*, *J* = 7.9, 1.2, H–C(8)); 7.46 (*dd*, *J* = 7.9, 1.2, H–C(6)); 7.35 (*t*, *J* = 7.9, H–C(7)); 6.91 (*dd*, *J* = 8.6, 2.0, H–C(2)); 6.88 (*d*, *J* = 2.0, H–C(4)); 3.96 (*s*, MeO). ^{13}C-NMR ((D$_6$)DMSO): 174.8 (C=O); 164.1 (C(3)); 157.4 (C(4a)); 148.2 (C(5)); 145.7 (C(4b)); 128.0 (C(1)); 123.8 (C(7)); 122.0 (C(8a)); 116.4 (C(8)); 115.9 (C(6)); 114.4 (C(2)); 113.9 (C(8b)); 102.24 (C(4)); 55.2 (MeO).

1-Hydroxy-3-methoxyxanthone (**13**). Obtained by demethylation from **14** according to the procedure described in [54]. M.p. 143–145°. IR (KBr): 3510, 1651, 1601, 1570, 1466. ^{1}H-NMR ((D$_6$)DMSO: 12.80 (*s*, OH); 8.15 (*dd*, *J* = 7.9, 1.7, H–C(8)); 7.88 (*ddd*, *J* = 7.9, 7.1, 1.7, H–C(6)); 7.61 (*dd*, *J* = 7.9, 1.7, C(5)); 7.49 (*ddd*, *J* = 7.9, 7.1, 1.7, H–C(7)); 6.67 (*d*, *J* = 2.3, C(4)); 6.42 (*d*, *J* = 2.3, H–C(2)); 3.88 (*s*, MeO). ^{13}C-NMR ((D$_6$)DMSO): 180.2 (C=O); 166.7 (C(3)); 162.6 (C(1)); 157.3 (C(4a)); 155.5 (C(4b)); 135.9 (C(6)); 125.3 (C(8)); 124.6 (C(7)); 119.9 (C(8a)); 117.8 (C(5)); 105.2 (C(8b)); 97.2 (C(2)); 92.9 (C(4)); 56.2 (MeO).

1,3-Dimethoxyxanthone (**14**). Obtained from salicylic acid and 1,3,5-trimethoxybenzene according to the procedure described in [53]. M.p. 170–172°. IR (KBr): 1651, 1601, 1466. ^{1}H-NMR ((D$_6$)DMSO): 8.06 (*dd*, *J* =

7.7, 1.7, H–C(8)); 7.75 (*ddd*, *J* = 7.9, 7.0, 1.8, H–C(6)); 7.51 (*dd*, *J* = 7.9, 1.8, C(5)); 7.39 (*ddd*, *J* = 7.9, 7.0, 1.8, H–C(7)); 6.69 (*d*, *J* = 2.2, C(4)); 6.50 (*d*, *J* = 2.2, H–C(2)); 3.90 (*s*, MeO); 3.86 (*s*, MeO). ^{13}C-NMR ((D$_6$)DMSO, 200 MHz): 180.0 (C=O); 164.8 (C(3)); 161.5 (C(1)); 159.1 (C(4a)); 154.3 (C(4b)); 134.3 (C(6)); 125.9 (C(8)); 124.1 (C(7)); 122.4 (C(8a)); 117.2 (C(5)); 107.9 (C(8b)); 95.4 (C(2)); 93.2 (C(4)); 56.2 (MeO); 56.0 (MeO).

3,5-Dimethoxyxanthone (**15**). Obtained from 3-methoxysalicylic acid and 1,3-dimethoxybenzene according to the procedure described in [53]. M.p. 173–175°. IR (KBr): 1650, 1616, 1485. ^{1}H-NMR ((D$_6$)DMSO): 8.09 (*d*, *J* = 8.9, H–C(1)); 7.7 (*dd*, *J* = 7.9, 1.7, H–C(8)); 7.49 (*dd*, *J* = 7.9, 1.7, H–C(6)); 7.38 (*t*, *J* = 7.9, H–C(7)); 7.20 (*d*, *J* = 2.4, H–C(4)); 7.05 (*dd*, *J* = 8.8, 2.4, H–C(2)); 3.97 (*s*, MeO–C(5)); 3.94 (*s*, MeO–C(3)). ^{13}C-NMR ((D$_6$)DMSO): 175.0 (C=O); 165.0 (C(3)); 157.4 (C(4a)); 148.3 (C(5)); 145.8 (C(4b)); 127.5 (C(1)); 124.0 (C(7)); 122.0 (C(8a)); 116.4 (C(8)); 116.1 (C(6)); 114.8 (C(2)); 114.1 (C(8b)); 100.6 (C(4)); 56.2 (2 MeO).

3,4-Dimethoxyxanthone (**19**), *3-Hydroxy-4-methoxyxanthone* (**18**), *and 4-Hydroxy-3-methoxyxanthone* (**17**). The xanthones **19**, **18**, and **17** were obtained from 2-hydroxy-2′,3,4-trimethoxybenzophenone, which was synthesized from the building blocks 2-methoxybenzoyl chloride and 1,2,3-trimethoxybenzene according to the procedure described in [40]. The xanthone **17** was also obtained by demethylation of **19** according to the procedure described in [55].

Compound **19**. M.p. 156–158° ([56]: 158–159° (petroleum)). IR (KBr): 1660, 1605, 1510, 1455, 1290, 1225, 1090, 750, 690. ^{13}C-NMR ((D$_6$)DMSO): 8.16 (*dd*, *J* = 7.9, 1.7, H–C(8)); 7.94 (*d*, *J* = 9.0, H–C(1)); 7.85 (*ddd*, *J* = 8.1, 7.5, 1.7, H–C(6)); 7.69 (*d*, *J* = 8.1, H–C(5)); 7.47 (*dd*, *J* = 7.9, 7.5, H–C(7)); 7.26 (*d*, *J* = 9.0, H–C(2)); 3.97 (*s*, MeO–C(3)); 3.92 (*s*, Me–C(4)). The ^{1}H-NMR data are in agreement with those given in [41]. ^{13}C-NMR ((D$_6$)DMSO): 175.3 (C(9)); 157.5 (C(3)); 155.6 (C(4b)); 149.9 (C(4a)); 135.9 (C(4)); 135.2 (C(6)); 125.9 (C(8)); 124.4 (C(7)); 121.7 (C(1)); 120.8 (C(8a)); 118.2 (C(5)); 115.9 (C(8b)); 109.7 (C(2)); 60.9 (*Me*O–C(4)); 56.1 (MeO–C(3)). The ^{13}C-NMR data are in agreement with those given in [41], except for C(3) and C(4b) for which the chemical shifts are interchanged. MS: 258 (2, $[M+2]^{+\cdot}$), 257 (18, $[M+1]^{+\cdot}$), 256 (100, $M^{+\cdot}$), 242 (8), 241 (43), 214 (4), 213 (24), 185 (5), 170 (16), 139 (3), 128 (4), 114 (11), 113 (3), 76 (6).

Compound **17**. M.p. 194–196°. IR (KBr): 3250, 1630, 1605, 1465, 1450, 1330, 1280, 1225, 1080, 900, 750. ^{1}H-NMR ((D$_6$)DMSO): 9.66 (*s*, OH); 8.16 (*dd*, *J* = 7.8, 1.7, H–C(8)); 7.84 (*ddd*, *J* = 8.3, 7.6, 1.7, H–C(6)); 7.68 (*d*, *J* = 9.0, H–C(1)); 7.65 (*dd*, *J* = 8.3, 1.0, H–C(5)); 7.44 (*ddd*, *J* = 7.8, 7.6, 1.0, H–C(7)); 7.19 (*d*, *J* = 9.0, H–C(2)); 3.96 (*s*, MeO). ^{13}C-NMR ((D$_6$)DMSO): 175.6 (C(9)); 155.7 (C(4b)); 152.5 (C(3)); 145.5 (C(4a)); 135.1 (C(6)); 134.1 (C(4)); 126.0 (C(8)); 124.1 (C(7)); 120.8 (C(8a)); 118.1 (C(5)); 116.3 (C(1)); 115.9 (C(8b)); 109.0 (C(2)); 56.4 (MeO). MS: 244 (2, $[M+2]^{+\cdot}$), 243 (17, $[M+1]^{+\cdot}$), 242 (100, $M^{+\cdot}$), 228 (4), 227 (28), 213 (3), 199 (14), 171 (11), 121 (4), 115 (9).

Compound **18**. M.p. 221–222° ([18]: 220–221°). IR (KBr): 3220, 1640, 1595, 1470, 1450, 1435, 1340, 1230, 1200, 1070, 1020, 745, 690. ^{1}H-NMR ((D$_6$)DMSO): 10.79 (*s*, OH); 8.16 (*dd*, *J* = 7.7, 1.7, H–C(8)); 7.84 (*ddd*, *J* = 8.1, 7.6, 1.7, H–C(6)); 7.80 (*d*, *J* = 8.9, H–C(1)); 7.69 (*dd*, *J* = 8.1, 1.0, H–C(5)); 7.46 (*ddd*, *J* = 7.7, 7.6, 1.0, H–C(7)); 7.00 (*d*, *J* = 8.9, H–C(2)); 3.92 (*s*, MeO). The ^{1}H-NMR data are in agreement with those given in [56]. ^{13}C-NMR ((D$_6$)DMSO): 175.0 (C(9)); 156.3 (C(3)); 155.5 (C(4b)); 150.7 (C(4a)); 135.0 (C(6)); 134.6 (C(4)); 125.9 (C(8)); 124.3 (C(7)); 121.6 (C(1)); 120.9 (C(8a)); 118.2 (C(5)); 114.8 (C(8b)); 114.1 (C(2)); 60.9 (MeO). MS: 244 (2, $[M+2]^{+\cdot}$), 243 (15, $[M+1]^{+\cdot}$), 242 (100, $M^{+\cdot}$), 228 (16), 227 (76), 213 (4), 200 (3), 199 (18), 171 (14), 121 (6), 115 (13), 114 (4).

2,3,4-Trimethoxyxanthone (**20**). Obtained according to the procedure described in [40]. M.p. 156–158° (from EtOH). IR (KBr): 2970, 1665, 1615, 1605, 1595, 1465, 1420, 1375, 1260, 1130.

The following compounds have been already described according to the references indicated: *1,3-dihydroxy-2-methylxanthone* (**26**) according to [57], *4-chloro-1,3-dihydroxy-2-methylxanthone* (**27**) according to [25], *4-bromo-1,3-dihydroxy-2-methylxanthone* (**28**) according to [25].

REFERENCES

[1] C. Altomare, P. A. Carrupt, P. Gaillard, N. El Tayar, B. Testa, A. Carotti, *Chem. Res. Toxicol.* **1992**, *5*, 366.
[2] Y. Tsugeno, A. Ito, *J. Biol. Chem.* **1997**, *272*, 14033.
[3] J. A. Moron, M. Campillo, V. Perez, M. Unzeta, L. Pardo, *J. Med. Chem.* **2000**, *43*, 1684.
[4] E. Kyburz, *Drug News Persp.* **1990**, *3*, 592.
[5] M. E. Bembenek, C. W. Abell, L. A. Chrisey, M. D. Rozwadowska, W. Gessner, A. Brossi, *J. Med. Chem.* **1990**, *33*, 147.
[6] M. Strolin Benedetti, P. L. Dostert, *J. Neural Transm.* **1987**, *23*, 103.

[7] F. Mazouz, S. Gueddari, C. Burstein, D. Mansuy, R. Milcent, *J. Med. Chem.* **1993**, *36*, 1157.
[8] H. L. White, P. Scates, *Drug Dev. Res.* **1992**, *25*, 191.
[9] O. Suzuki, Y. Katsumata, M. Oya, V. M. Chari, B. Vermes, H. Wagner, K. Hostettmann, *Planta Med.* **1981**, *42*, 17.
[10] K. Hostettmann, M. Hostettmann, in 'Methods In Plant Biochemistry', Ed. Y. B. Harborne, Academic Press, New York, 1989, pp. 493 – 508.
[11] B. Shearer, J. Sullivan, J. Carter, R. Mathew, P. Waid, J. Connor, R. Patch, J. Burch, *J. Med. Chem.* **1991**, *34*, 2931.
[12] V. Rovei, D. Caille, O. Curet, D. Ego, F. X. Jarreau, *J. Neural Transm.* **1994**, *41*, 339.
[13] F. Moureau, J. Wouters, D. P. Vercauteren, S. Collin, G. Evrard, F. Durant, F. Ducrey, J. J. Koenig, F. X. Jarreau, *Eur. J. Med. Chem.* **1994**, *29*, 269.
[14] M. J. Laughton, P. J. Evans, M. A. Moroney, J. R. S. Hoult, B. Halliwell, *Biochem. Pharmacol.* **1991**, *42*, 1673.
[15] T. A. Halgren, *J. Comput. Chem.* **1996**, *17*, 520.
[16] GAUSSIAN 98 software (Revision A.1). M. J. Frish, G. W. Trucks, H. B. Schelgel, M. A. Scuseria, M. A. Robb, J. R. Cheeseman, V. G. Zahrzewski, J. A. Montgomery, R. E. Stratmann, J. C. Burant, S. Dapprich, J. M. Millam, A. D. Daniels, K. N. Kudin, M. C. Strain, O. Farkas, J. Tomasi, V. Barone, M. Cossi, R. Cammi, B. Mennucci, C. Pomelli, C. Adamo, S. Clifford, J. Ochterski, G. A. Petersson, P. Y. Ayala, Q. Cui, K. Morokuma, D. K. Malick, A. D. Rabuck, K. Raghavachari, J. B. Foresman, J. Cioslowski, J. V. Ortiz, B. B. Stefanov, G. Liu, A. Liashenko, P. Piskorz, I. Komaromi, R. Gomperts, R. L. Martin, D. J. Fox, T. Keith, M. A. Al-Laham, C. Y. Peng, A. Nanayakkara, C. Gonzalez, M. Challacombe, P. M. W. Gill, B. G. Johnson, W. Chen, M. W. Wong, J. L. Andres, M. Head-Gordon, E. S. Replogle, J. A. Pople. Pittsburgh PA, Copyright(©) 1998, Gaussian, Inc., 1998.
[17] P. Gaillard, P. A. Carrupt, B. Testa, A. Boudon, *J. Comput.-Aided Mol. Design* **1994**, *8*, 83.
[18] Almond 2.0. Multivariate Infometric Analysis, Perugia, Italy, 1999.
[19] Grid1.7. Molecular Discovery Ltd, West Way House, Elms Parade, Oxford OX2 9LL, 1999.
[20] GOLPE 4.5. Multivariate Infometric Analysis, Perugia, Italy, 1999.
[21] Tsar 3.0. Oxford Molecular Ltd., Oxford, UK, 1997.
[22] H. Weissbach, T. E. Smith, J. W. Daly, B. Witkop, S. Udenfriend, *J. Biol. Chem.* **1960**, *235*, 1160.
[23] S. Kneubühler, U. Thull, C. Altomare, V. Carta, P. Gaillard, P. A. Carrupt, A. Carotti, B. Testa, *J. Med. Chem.* **1995**, *38*, 3874.
[24] P. J. F. Henderson, in 'Techniques in the Life Sciences, B1/II Supplement, Protein and Enzyme Biochemistry', Ed. K. F. Tipton, Elsevier, Dublin, 1985, pp. 1 – 48.
[25] U. Thull, S. Kneubühler, B. Testa, M. F. M. Borges, M. M. M. Pinto, *Pharm. Res.* **1993**, *10*, 1187.
[26] V. Glover, J. Liebowitz, I. Armando, M. Sandler, *J. Neural Transm.* **1982**, *54*, 209.
[27] P. L. Dostert, E. M. O'Brien, K. F. Tipton, M. Meroni, P. Melloni, M. Strolin Benedetti, *Eur. J. Med. Chem.* **1992**, *27*, 45.
[28] A. Codoner, I. S. Monzo, C. Ortiz, A. Olba, *J. Chem. Soc., Perkin Trans. 2* **1989**, 107.
[29] M. Baroni, G. Costantino, G. Cruciani, D. Riganelli, R. Valigi, S. Clementi, *Quant. Struct.-Act. Relat.* **1993**, *12*, 9.
[30] J. L. Wolfender, M. Hamburger, J. D. Msonthi, K. Hostettmann, *Phytochemistry* **1991**, *30*, 3625.
[31] L. Rocha, A. Marston, M. A. C. Kaplan, H. Stoeckli-Evans, U. Thull, B. Testa, K. Hostettmann, *Phytochemistry* **1994**, *36*, 1381.
[32] I. Sordat-Diserens, C. Rogers, B. Sordat, K. Hostettmann, *Phytochemistry* **1992**, *31*, 313.
[33] I. Sordat-Diserens, M. Hamburger, C. Rogers, K. Hostettmann, *Phytochemistry* **1992**, *31*, 3589.
[34] D. Schaufelberger, K. Hostettmann, *Planta Med.* **1987**, *54*, 219.
[35] I. Sordat-Diserens, A. Marston, M. Hamburger, C. Rogers, K. Hostettmann, *Helv. Chim. Acta* **1989**, *72*, 1001.
[36] A. Bashir, M. Hamburger, J. D. Msonthi, K. Hostettmann, *Phytochemistry* **1992**, *31*, 309.
[37] A. Bashir, M. Hamburger, M. P. Gupta, P. Solis, K. Hostettmann, *Phytochemistry* **1992**, *31*, 3203.
[38] M. C. Recio-Iglesias, A. Marston, K. Hostettmann, *Phytochemistry* **1992**, *31*, 1387.
[39] W. G. Ma, N. Fuzzati, Q. S. Li, C. R. Yang, K. Hostettmann, H. Stoeckli-Evans, *Phytochemistry* **1995**, *39*, 1049.
[40] A. J. Quillinan, F. Scheinmann, *J. Chem. Soc., Perkin Trans. 1* **1973**, 1329.
[41] C. N. Lin, S. S. Liou, F. N. Ko, C. M. Teng, *J. Pharm. Sci.* **1993**, *82*, 11.
[42] R. A. Finnegan, P. L. Bachmann, *J. Pharm. Sci.* **1965**, *54*, 633.
[43] J. E. Atkinson, J. R. Lewis, *J. Chem. Soc. (C)* **1969**, 281.

[44] F. D. Monache, M. M. Mac-Quhae, G. D. Monache, G. B. M. Bettolo, R. A. Lima, *Phytochemistry* **1983**, *22*, 227.
[45] P. W. Westerman, S. P. Gunasekera, M. Uvais, S. Sultanbawa, R. Kazlauskas, *Org. Magn. Reson.* **1977**, *9*, 631.
[46] A. W. Frahm, R. K. Chaudhuri, *Tetrahedron* **1979**, *35*, 2035.
[47] D. B. Boyd, in 'Reviews in Computational Chemistry', Eds. K. B. Lipkowitz and D. B. Boyd, VCH Publishers, New York, 1995, Vol. 6, pp. 317–382.
[48] R. K. Chaudhuri, F. Zymalkowski, A. W. Frahm, *Tetrahedron* **1978**, *34*, 1837.
[49] R. A. Finnegan, J. K. Patel, *J. Chem. Soc., Perkin Trans. 1* **1972**, 1896.
[50] J. L. Okogun, *J. Chem. Soc., Perkin Trans. 1* **1976**, *21*, 2241.
[51] R. C. Young, R. C. Mitchell, T. H. Brown, C. R. Ganellin, R. Griffiths, M. Jones, K. K. Rana, D. Saunders, I. R. Smith, N. E. Sore, T. J. Wilks, *J. Med. Chem*. **1988**, *31*, 656.
[52] R. Royer, J. Lechartier, P. Demerseman, *Bull. Soc. Chim. Fr.* **1971**, 1707.
[53] P. K. Grover, G. D. Shah, R. C. Shah, *J. Chem. Soc*. **1955**, 3982.
[54] T. Sargi, *Tetrahedron* **1996**, *52*, 13623.
[55] O. R. Gottlieb, A. A. L. Mesquita, G. G. Oliveira, M. T. Melo, *Phytochemistry* **1970**, *9*, 2535.
[56] S. P. Gunasekera, S. Ramachandran, S. Selliah, M. U. S. Sultanbawa, *J. Chem. Soc., Perkin Trans. 1* **1975**, *1*, 2447.
[57] M. M. M. Pinto, J. Polonia, *Helv. Chim. Acta* **1974**, *57*, 2613.

Received October 28, 2000